

## Synthesis and characterization of aminated SiO<sub>2</sub>/CoFe<sub>2</sub>O<sub>4</sub> nanoparticles

XIAO Xu-xian(肖旭贤)<sup>1</sup>, HUANG Ke-long(黄可龙)<sup>1</sup>, HE Qiong-qiong(何琼琼)<sup>2</sup>

1. School of Chemistry and Chemical Engineering, Central South University, Changsha 410083, China;

2. School of Basic Medical Sciences, Central South University, Changsha 410013, China

Received 23 April 2007; accepted 28 June 2007

**Abstract:** A kind of newly aminated CoFe<sub>2</sub>O<sub>4</sub> nanoparticles were synthesized by grafting process for biomedical applications, which were coated primarily with silicon dioxide(SiO<sub>2</sub>). The characterizations of aminated SiO<sub>2</sub>/CoFe<sub>2</sub>O<sub>4</sub>(ASCN) and SiO<sub>2</sub>-coated CoFe<sub>2</sub>O<sub>4</sub>(SCN) nanoparticles were investigated using elemental analysis, thermogravimetric analysis(TGA), differential thermal analysis(DTA), infrared spectroscopy(IR), atomic force microscopy(AFM), zeta-potential measurement and vibrating sample magneto-metry(VSM). The AFM micrograph shows that the ASCN nanoparticles are approximately spherical with an average diameter of 30 nm. Based on IR and TGA results, it is suggested that the surface of the SiO<sub>2</sub>-coated CoFe<sub>2</sub>O<sub>4</sub> nanoparticles are grafted with amino compounds. The elemental analysis also shows the presence of 0.98 mmol/g of organic moieties immobilized on the surface of ASCN nanoparticles. Zeta-potential data of ASCN nanoparticles also reveal that amino compounds are bonded onto the surface of SiO<sub>2</sub>-coated CoFe<sub>2</sub>O<sub>4</sub> nanoparticles by ether linkage. The magnetic parameters show that ASCN nanoparticles still have good magnetic property.

**Key words:** cobalt ferrites; nanoparticles; magnet; amination; graft; zeta potential; surface modification

### 1 Introduction

Recently, nanometer-sized ferrite particles are regarded as a class of important magnetic materials, which have attracted the attention of many researchers, due to their large surface-to-volume ratio, quantum-size effect, superior magnetic character and catalytic activity as well as their potential application in many domains. Various ferrite nanoparticles of different chemical compositions, shapes and size distributions have been prepared by different methods, such as co-precipitation method[1–2], shock wave treatment[3], sol-gel process [4–5], hydrothermal process[6–7], microemulsion approach[8–9]. For example, XU et al[10] synthesized nanoparticles by combustion method, SHAP and PILLAI[11] prepared the precursor of CoFe<sub>2</sub>O<sub>4</sub> by microemulsion approach, and these precursors were then calcined to give CoFe<sub>2</sub>O<sub>4</sub> nanoparticles. In our laboratory, the CoFe<sub>2</sub>O<sub>4</sub> nanoparticles were synthesized by using a new reverse microemulsion system consisting of water (or brine)/ TX-10, AEO9/cyclohexane/*n*-pentanol[12].

With the development of nanoparticles technology and biomedical science, the technology of nanoparticle therapy was put forward in time. One major hurdle that underlies the use of nanoparticle therapy is how to get the nanoparticles to a particular site in the body. Magnetic nanoparticles have been proposed for use as biomedical purposes for several years, for which a potential benefit is the use of localized magnetic field gradients to attract the particles to a targeted site until the therapy is complete and then to remove them. However, the agglomeration, toxicity and poor biocompatibility of bare ferrite nanoparticles restrict their application. Surface modification of ferrite nanoparticles is crucial because it can improve the stability, biocompatibility and biodistribution. To date a wide variety of modifying materials such as oleic acids, silicons, aminosilane, poly(ethylene glycol), chitosan[13] have been used to improve chemical stability and biocompatibility of magnetite for various biomedical applications. But to the best of our knowledge, no report has yet been published using alkamine as a modifying material of magnetic nanoparticles for the application of gene delivery.

In this study, the  $\text{CoFe}_2\text{O}_4$  nanoparticles is primarily coated with silicon dioxide by sol-gel process, and low relative molecular mass alkamine molecules due to its low toxicity are grafted onto the surface of  $\text{SiO}_2$ -coated  $\text{CoFe}_2\text{O}_4$  nanoparticles. The newly aminated  $\text{SiO}_2/\text{CoFe}_2\text{O}_4$  nanoparticles(ASCN) are characterized by elemental analysis, TGA-DTA, AFM, IR, zeta-potential measurement and VSM techniques.

## 2 Experimental

### 2.1 Materials

Unless otherwise noted, all reagents were from Hunan Chemical Co. DMF, benzene, pyridine, thionyl chloride, and 3-(Fmoc-amino)-1-propanol ( $\geq 98.0\%$ ) were in analytic grades, isooctane and pyridine were distilled over  $\text{CaH}_2$  before use. Pyridine was further purified by freeze-pump-thaw cycles on a vacuum line. Silica coated magnetic nanoparticle was prepared in our laboratory.

### 2.2 Chlorination of silanol groups with thionyl chloride

Silica coated magnetic nanoparticle (6.0 g) was added into a dry 250 mL round-bottom flask equipped with a reflux condenser and a magnetic stirrer. Thionyl chloride (50 mL) was charged followed by the addition of 50 mL benzene. The mixture was stirred and refluxed for 50 h. After the reaction, unreacted thionyl chloride and benzene were removed by distillation and drying at  $90\text{ }^\circ\text{C}$  in vacuum for 24 h. The treated nanoparticles (Compound 1, C1) were stored in a desiccator in vacuum.

### 2.3 Alkamine reaction with chlorinated surface

3-(Fmoc-amino)-1-propanol solution (0.1 mol/L in DMF, with 0.01 mol/L pyridine) was transferred to the reaction flask via a metal cannula. Each sample was completely immersed in the solution and kept under argon. The reaction time was longer than 48 h at the temperature of  $80\text{ }^\circ\text{C}$ . After the reaction, the samples (Compound 2, C2) were removed from the DMF solution, rinsed extensively with  $\text{CH}_2\text{Cl}_2$ . The Fmoc blocking group was removed in 20% piperidine in DMF. After deprotection, the product was washed with excess boiling toluene and Soxhlet extract in  $\text{CH}_2\text{Cl}_2$ . In the end, the aminated  $\text{SiO}_2/\text{CoFe}_2\text{O}_4$ (ASCN) nanoparticles (Compound 3, C3) were obtained.

### 2.4 Characterization

Thermogravimetric analysis(TGA) and differential thermal analysis(DTA) were performed on a Hi-Res SDT 2960 model thermal analyzer. The heating rate for TGA

and DTA was  $5\text{ }^\circ\text{C}/\text{min}$  and the range was from  $20\text{ }^\circ\text{C}$  to  $500\text{ }^\circ\text{C}$ . The infrared spectra of all nanoparticles products in KBr wafers were recorded with an infrared spectrophotometer (IR, Nicolet, 750). A nanoscope III atomic force microscope(AFM) was also used for the observation of their morphology. The silica coated magnetic nanoparticles and alkamine grafted magnetic nanoparticles were characterized by quantitative elemental analysis (C and N analysis) using a Perkin-Elmer 2400 Series II micro-elemental analyzer.

The zeta potentials and particle distribution of samples were measured respectively by laser electrophoresis instrument (Laser Zee, Model 500, USA) and laser granulometry (CILAS 1064, France). The magnetic properties of the nanoparticles were measured using a vibrating sample magnetometer (VSM, VBH-55).

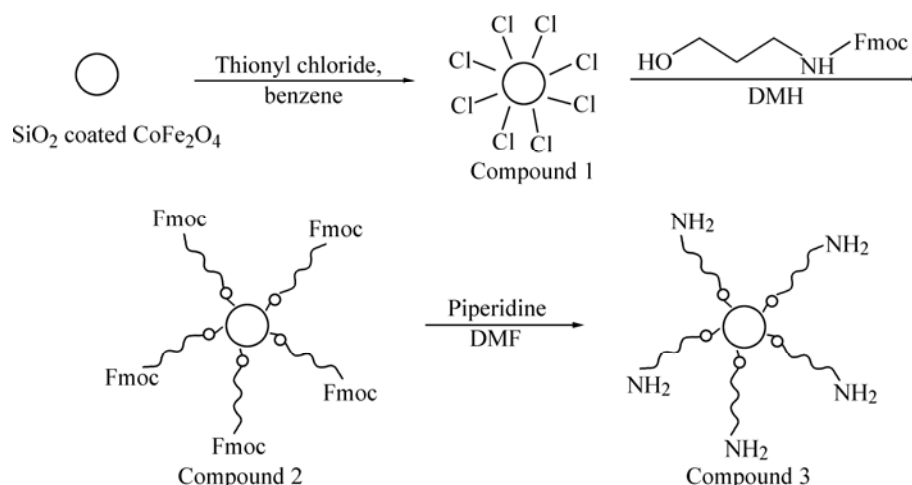
## 3 Results and discussion

Fig.1 shows the synthetic steps for forming hybrid organic-inorganic nanocomposite. In this study, the preparation of  $\text{SiO}_2$  coated  $\text{CoFe}_2\text{O}_4$  nanoparticles was according to Ref.[14]. The chlorination of silanol groups on silica coated magnetic particle was carried out according to a modified procedure[15]. The reaction of 3-(Fmoc-amino)-1-propanol with the chlorinated surfaces of nanoparticles was according to Ref.[16]. In the present report, we successfully synthesized the aminated  $\text{SiO}_2/\text{CoFe}_2\text{O}_4$  nanoparticles according to the reference method. Without any doubt, this method could also be used to prepare other nanoscaled organic molecule grafted metal oxide by grafting process.

The amount of the amino grafted onto the surface of  $\text{SiO}_2/\text{CoFe}_2\text{O}_4$  nanoparticles was determined by elemental analysis. From the contents of carbon and nitrogen in the samples, it is possible to calculate the amount of substance of the compounds attached onto surfaces, as listed in Table 1. The ratio of C/N for the sample C3 can be calculated as 2.57, which is consistent with the C/N ratio of a bonded unit of 3-amino propoxy molecules. In contrast, carbon and nitrogen elements are not found on the surface of the unmodified  $\text{SiO}_2/\text{CoFe}_2\text{O}_4$  nanoparticles. These results indicate that alkamine molecule is successfully grafted onto the surface of the  $\text{SiO}_2/\text{CoFe}_2\text{O}_4$  nanoparticles.

**Table 1** Elements analysis of carbon and nitrogen for unmodified  $\text{SiO}_2$ -coated  $\text{CoFe}_2\text{O}_4$  and aminated  $\text{SiO}_2/\text{CoFe}_2\text{O}_4$  (ASCN) nanoparticles and immobilized amount(Q)

Sample	$x(\text{C})/\%$	$x(\text{H})/\%$	$x(\text{N})/\%$	$Q/(\text{mmol}\cdot\text{g}^{-1})$
Unmodified	—	—	—	—
C2	9.24	0.775	0.598	0.427
C3	1.50	0.335	0.582	0.416



**Fig.1** Synthetic steps of aminated magnetic nanoparticles

The typical TG-DTA result for the inorganic-organic materials is shown in Fig.2. The mass loss is mainly divided into two temperature regions: below 100 °C and 200–400 °C. The mass loss below 100 °C is due to the evaporation of solvent and loosely bound water molecules trapped in the materials, supporting by the presence of an endothermic peak at 100 °C in DTA. Between 200 and 400 °C there are two regions of mass loss associated with two exothermic DTA peaks, which correspond to different stages in the oxidation of the organic species. Two peaks are observed at approximately 230 and 360 °C, respectively. The former is ascribed to the decomposing reaction of organic modifier. The latter corresponds to the combustion of organic residuals, which is approximately equal to the mass fraction of the organic materials on the surface of the silica/CoFe<sub>2</sub>O<sub>4</sub> nanoparticles. However, only one mass loss period below 100 °C is observed for unmodified silica/CoFe<sub>2</sub>O<sub>4</sub> nanoparticles. It reveals that there are no organic molecules on the surface of nanoparticles.

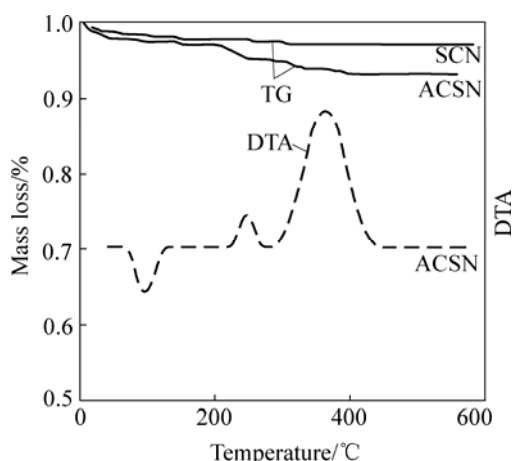


**Fig.2** TG/DTA plots of ACSN and TG plot of SCN

There are some notable differences between the IR spectrum of SiO<sub>2</sub> coated CoFe<sub>2</sub>O<sub>4</sub> nanoparticles and that of the ASCN nanoparticles shown in Fig.3. For two nanoparticles, two absorption peaks appear in the spectra, which are related to the characteristic vibrational transverse optical modes of Si—O—Si chemical bond. The band, which appears near 452 cm<sup>-1</sup>, is the rocking vibrational mode. The absorption band near about 796 cm<sup>-1</sup> corresponds to the bending vibration of Si—O—Si bond. For ASCN nanoparticles, they possess absorption bands in 2 928.8 and 2 852.5 cm<sup>-1</sup> due to stretching vibration of C—H bond. The peaks at 1 620 cm<sup>-1</sup> and 885.2 cm<sup>-1</sup> are due to the deformation and bending vibration modes of —NH<sub>2</sub> group. In addition, the absorption bands of ASCN near 3 400 cm<sup>-1</sup> due to the vibration of remainder H<sub>2</sub>O in the sample becomes smaller, and the band near 3 400 cm<sup>-1</sup> due to the stretching vibration of —NH<sub>2</sub> group is observed. But for SCN nanoparticles, the absorption bands of C—H bond and —NH<sub>2</sub> group are not observed. These results indicate

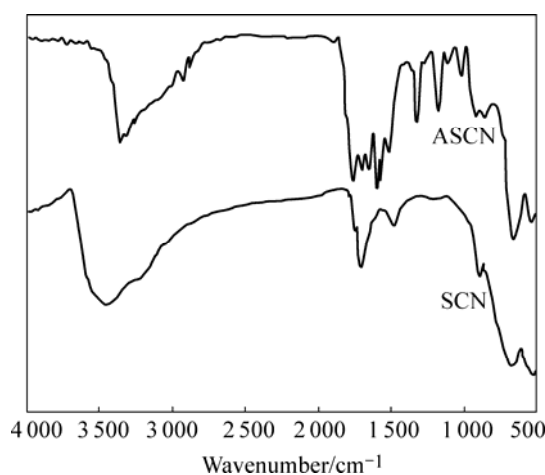


**Fig.3** IR spectra of unmodified and ASCN samples

successful covalent linkage of the amino functional group to the  $\text{SiO}_2$  substrate.

The surface morphologies and the size of SCN and ASCN nanoparticles can be directly observed with AFM. In Fig.4(a), the SCN particles are monodisperse and nearly spherical in shape. The average size is about 25 nm in diameter, and they have a smooth surface. The narrow particle size distribution is shown in Fig.5(a). The AFM image in Fig.4(b) shows that the amino grafted nanoparticles also remain monodisperse and spherical with the average diameter of 30 nm, and the surface of the amino grafted nanoparticles is rougher than that of the SCN nanoparticles. A very broad particle size distribution is shown in Fig.5(b). Prolonged Soxhlet extraction has no effect on the rough surface topography, indicating that the remaining organic matter is covalently linked to the surface of  $\text{SiO}_2$  coated  $\text{CoFe}_2\text{O}_4$  nanoparticles and any loosely bound organic chains are completely removed by the treatment. The reason of the difference can be attributed to the amino molecule grafting onto the surface of nanoparticles.

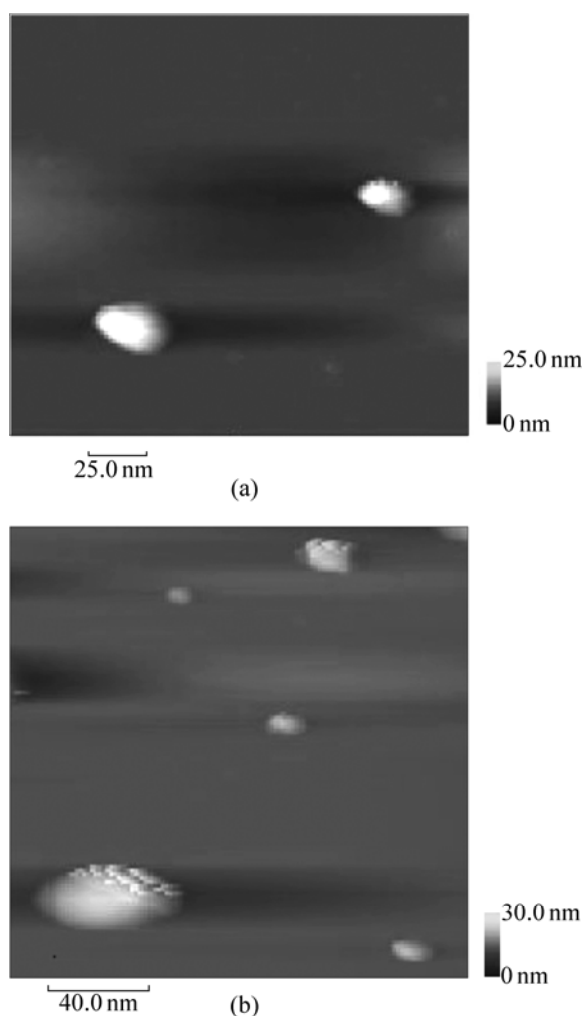


**Fig.4** AFM micrographs of unmodified (a) and ASCN(b) samples

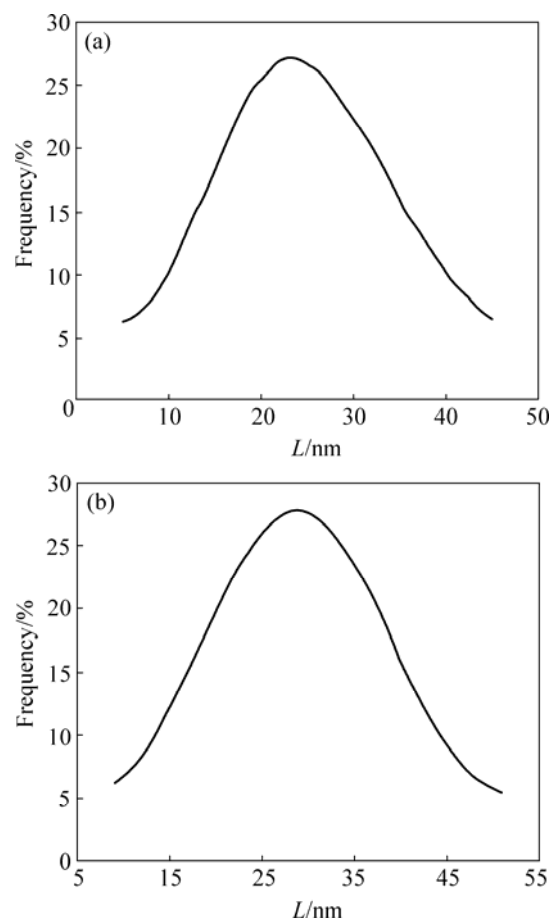


**Fig.5** Size distribution of unmodified SCN (a) and ASCN (b) nanoparticles

Fig.6 shows the zeta potential data for two samples. The isoelectric point (iep) is defined as the pH value at which the zeta potential is zero. The isoelectric points of the nanoparticles are: pH 2.2 for  $\text{SiO}_2$ -coated  $\text{CoFe}_2\text{O}_4$  nanoparticles, pH 9.8 for ASCN nanoparticles. It is clear that zeta potential of  $\text{SiO}_2$ -coated  $\text{CoFe}_2\text{O}_4$  nanoparticles is similar to the zeta potential of silica[17], and it is different from the zeta potential of ASCN nanoparticles.

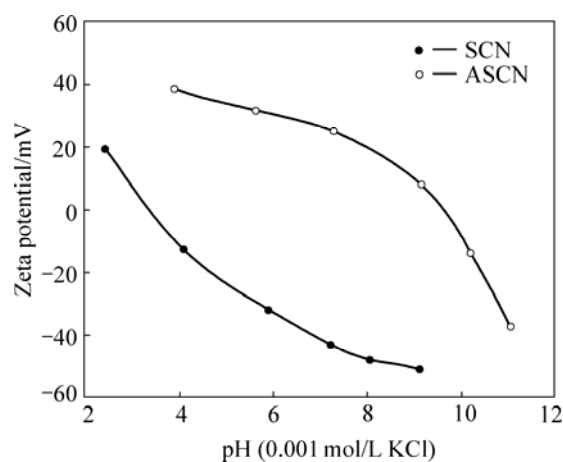


**Fig.6** Zeta potential of samples as function of pH value

In this case, iep is shifted toward higher pH values. On the basis of this fact, it is considered that organic molecules form as thin films on the SiO<sub>2</sub>-coated CoFe<sub>2</sub>O<sub>4</sub> cores.

The magnetic properties of the ASCN and SiO<sub>2</sub>-coated Co ferrite nanoparticles were measured at room temperature by VSM, as shown in Fig.7. They exhibit typical superparamagnetic behavior. The magnetization of ASCN nanoparticles is lower than that of SiO<sub>2</sub>-coated Co ferrite nanoparticles. This might be due to the amorphous character and thickness of organic moieties on the surface of nanoparticles. This reduction in magnetization also might be due to the difference in nanoparticle size and the accompanied change in surface area.

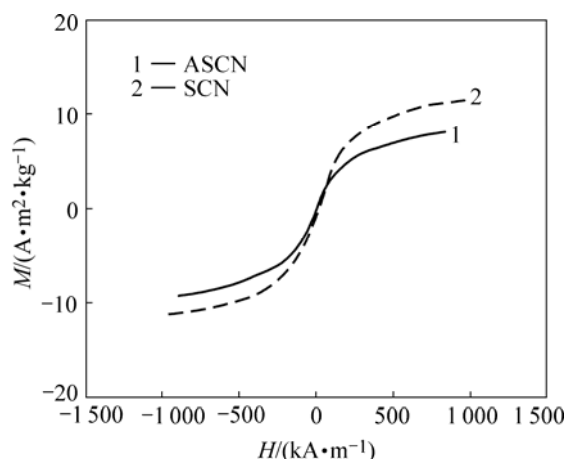


**Fig.7** Magnetization curves of unmodified SCN and ASCN nanoparticles

## 4 Conclusions

1) The elemental analysis and thermogravimetric analysis of ASCN nanoparticles show the presence of organic moieties immobilized on the surface of ASCN nanoparticles.

2) AFM results indicate that nanoparticles are approximately spherical, regular and in the size range of 20–40 nm, which have a very broad particle size distribution.

3) IR absorption spectra show the ASCN nanoparticles have the characteristic bands of NH<sub>2</sub> group, while SiO<sub>2</sub> coated CoFe<sub>2</sub>O<sub>4</sub> nanoparticles have no characteristic bands of NH<sub>2</sub> group.

4) Modification of nanoparticles surface with amino compound also induces a clear shift in iep toward high pH values.

5) The aminated SiO<sub>2</sub>/CoFe<sub>2</sub>O<sub>4</sub> nanoparticles

(ASCN) present better magnetic behavior.

## References

- [1] MILLOT N, GALLET S LE, AYMES D, BERNARD F, GRIN Y. Spark plasma sintering of cobalt ferrite nanopowders prepared by coprecipitation and hydrothermal synthesis [J]. *Journal of the European Ceramic Society*, 2007, 27(2/3): 921–926.
- [2] YAMAMOTO H, ISONO M, KOBAYASHI T. Magnetic properties of Ba-Nd-Co system M-type ferrite fine particles prepared by controlling the chemical coprecipitation method [J]. *Journal of Magnetism and Magnetic Materials*, 2005, 295(1): 51–56.
- [3] LIU Jian-jun, HE Hong-liang, JIN Xiao-gang, HAO Zheng-ping, HU Zhuang-qi. Synthesis of nanosized nickel ferrites by shock waves and their magnetic properties [J]. *Materials Research Bulletin*, 2001, 36(13/14): 2357–2363.
- [4] AZADMANJIRI J, SALEHANI H K, BARATI M R, FARZAN F. Preparation and electromagnetic properties of Ni<sub>1-x</sub>Cu<sub>x</sub>Fe<sub>2</sub>O<sub>4</sub> nanoparticle ferrites by sol-gel auto-combustion method [J]. *Materials Letters*, 2007, 61(1): 84–87.
- [5] TIWARI S D, RAJEEV K P. Magnetic properties of NiO nanoparticles [J]. *Thin Solid Films*, 2006, 505(1/2): 113–117.
- [6] WANG Jun, ZENG Chuan, PENG Zhen-meng, CHEN Qian-wang. Synthesis and magnetic properties of Zn<sub>1-x</sub>Mn<sub>x</sub>Fe<sub>2</sub>O<sub>4</sub> nanoparticles [J]. *Physica B: Condensed Matter*, 2004, 349(1/4): 124–128.
- [7] MILLOT N, XIN B, PIGHINI C, AYMES D. Hydrothermal synthesis of nanostructured inorganic powders by a continuous process under supercritical conditions [J]. *Journal of the European Ceramic Society*, 2005, 25(12): 2013–2016.
- [8] LI Gui-juan, YAN Shi-feng, ZHOU En-le, CHEN Yan-mo. Preparation of magnetic and conductive NiZn ferrite polyaniline nanocomposites with core shell structure [J]. *Colloid Surface A*, 2006, 276(1/3): 40–44.
- [9] USKOKOVIĆ V, DROFENIK M. A mechanism for the formation of nanostructured NiZn ferrites via a micro emulsion-assisted precipitation method [J]. *Colloids and Surfaces A: Physicochemical and Engineering Aspects*, 2005, 266(1/3): 168–174.
- [10] XU Zhi-gan, CHENG Fu-xian, ZHOU Biao, LIAO Chun-sheng, YAN Chun-hua. Synthesis of CoFe<sub>2</sub>O<sub>4</sub> nanoparticles by combustion method and its characterization [J]. *Chinese Science Bulletin*, 2000, 45(17): 1837–1841.
- [11] SHAH D O, PILLAI V. Synthesis of high-coercivity cobalt ferrite particles using water-in-oil microemulsions [J]. *Journal of Magnetism and Magnetic Materials*, 1996, 163: 243–248.
- [12] XIAO Xu-xian, HUANG Ke-long, LU Lin-bing, SHANG Ju-qing. Preparation of CoFe<sub>2</sub>O<sub>4</sub> nanoparticles by microemulsion approach [J]. *J Cent South Univ*, 2005, 36(1): 65–68. (in Chinese)
- [13] KIM D H, LEE S H, IM K H, KIM K N, KIM K M, SHIM I B, LEE M H, LEE Y K. Surface-modified magnetite nanoparticles for hyperthermia: Preparation, characterization, and cytotoxicity studies [J]. *Current Applied Physics*, 2006, 6(s1): 242–246.
- [14] XIAO Xu-xian, HUANG Ke-long, YAN Jian-hui, HE Qiong-qiong. Synthesis and characterization of CoFe<sub>2</sub>O<sub>4</sub> nanoparticles [J]. *Trans Nonferrous Met Soc China*, 2005, 15(5): 1172–1177.
- [15] KATZ A, DA COSTA P, LAM A C P, NOTESTEIN J M. The first single-step immobilization of a Calix-[4]-arene onto the surface of silica [J]. *Chem Mater*, 2002, 14(8): 3364–3368.
- [16] RYAN C M, ZHU X Y. Two-step approach to the formation of organic monolayers on the silicon oxide surface [J]. *Langmuir*, 2001, 17(18): 5576–5580.
- [17] SADASIVAN S, RASMUSSEN DH, CHEN F P, KANNABIRAN R K. Preparation and characterization of ultrafine silica [J]. *Colloid Surface A*, 1998, 132(1): 45–52.

(Edited by YUAN Sai-qian)